

Preliminary Structural Design Of Regional Jetliner's Aileron

ABSTRACT

The preliminary structural design of ailerons in regional jet liners is essential because ailerons are critical control surfaces that enable the pilot to roll the airplane across its longitudinal direction. Ailerons are located on the trailing edge of the wing and are designed to create a differential lift between the wing's upper and lower surfaces, which generates a rolling moment that allows the aircraft to turn.

The preliminary structural design of ailerons involves determining the appropriate size, shape, and material for the aileron structure, ensuring that it is strong enough to withstand the loads that it will experience during flight. The design must also consider factors such as weight, aerodynamics, and maneuverability.

Ailerons are subjected to significant aerodynamic forces and loads during flight, so their structural design must be robust enough to withstand these loads without failing. If ailerons are not properly designed, they can fail, which can result in a loss of control of the aircraft, leading to a potentially catastrophic situation. Therefore, the preliminary structural design of ailerons is critical to ensure that the aircraft is safe to fly, and the pilot can control it effectively during all phases of flight.

Key words: Structural design, Regional jet liners, Aircraft, Wing's,

1. INTRODUCTION

The aileron located on the right wing deflects upward when [20-25] the flight deck right-hand movement of the steering wheel or control stick causes the left wing's aileron to deflect laterally at the same time. Right wing lift is lessened because of the right aileron's upward deflection since it lessens the wing's camber. On the other hand, the upward deflection of the left aileron increases camber, which in turn increases lift on the left wing. The airplane rolls to the right because of the difference in lift between the wings. Ailerons are roll spoilers are utilized as a complement on some aircraft. the wing's upper surface. There are three further primary aileron types: [1-6]

The Differential aileron is deployed more than the lowered aileron is lowered because differential ailerons are meant to work at separate rates. As a result, the down-moving wing experiences parasite drag, which is equal to the induced drag of the lifted wing. It helps, but the negative yaw is still present[26-28].

The Fraise aileron travels up, a little portion of the control surface likewise deflects downward to create extra drag. Once more, to balance

off the induced drag created on the other side, this design adds parasitic drag to the wingtip that is moving downhill.

The final kind of aileron design is when the rudder and ailerons have connected controls. A set of springs apply pressure to the rudder in the same direction as the pilot's ailerons when they are moved to the left or right. Although there is still adverse yaw, the linkage assists the pilot in reducing it by applying a small amount of rudder. [7-10]

2. PROTOTYPE REGIONAL AIRCRAFT AND SPECIFICATIONS

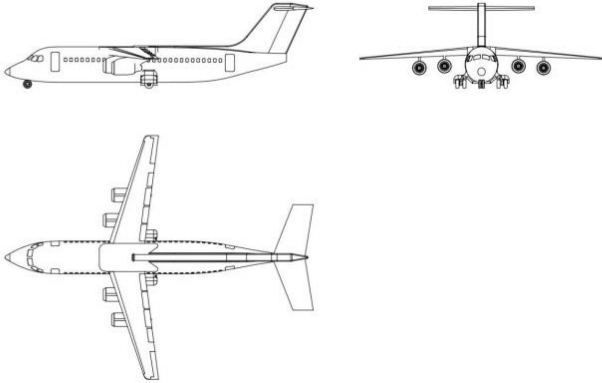


FIG 1 THE THREE-VIEW DRAWING OF THE PROTOTYPE

2.1 The Aerodynamic Layout

The aircraft has a traditional wing-tail aerodynamic configuration. The aircraft's horizontal and vertical tails are situated behind the wing, which is its most distinctive characteristic. The most significant a typical aerodynamic configuration for contemporary aircraft, which has significant benefits for flight stability and noise reduction. [11-14]

2.12 The Scheme of Aircraft Trimming in Flight

In steady horizontal flight, the aircraft lift is equal to the aircraft weight, the sum of the

moments of the centre of gravity

$$L = G; \Sigma m_y = 0$$

Which can be indicated as;

$$L_{wing} = G + L_{hor.tail}$$

$$L_{wing} \alpha = L_{hor.tail} l_{HT}$$

WHERE

$$L_{wing}$$

is the wing lift which equals to the aircraft lift minus horizontal tail lift;

G is the aircraft weight;

$$L_{hor.tail}$$

is the horizontal tail lift;

a is the distance between the wing centre of pressure CP and the aircraft centre of gravity CG;

L_{ht}

is the distance between centre of pressure CP of the horizontal tail and the aircraft centre

of gravity CG;

However, with wing-tail aircraft, the wing lift is larger than the aircraft weight by an amount equal to the horizontal tail's trimming force. The aircraft's angle of attack must be increased to produce wing lift, which raises the drag coefficient and lowers the aircraft's lift-to-drag ratio. These are the trim costs associated with the typical wing-tail design. Low-wing layouts, which are frequently employed on cargo/transport airliners, are characterized by the location of the wing in relation to the longitudinal axis of the aircraft. Each wing has a place for the two engines.

Pros;

- The engine may be maintained effortlessly in the lower position
- The installation of the landing gear allows for easier structural design
- the safety of the aircraft during an emergency landing
- Other components of the aircraft won't disrupt the engine's air intake;
- the wing's spar is located beneath the floor, it is simple to arrange the cabin.

Cons;

- The wing's junction with the fuselage is where there is most drag;
- Due of the wing's proximity to the ground, the engine is more susceptible to outside influences on the runway.

2.13 The Take-off Mass and Weight

The primary factor and technical requirement are the aircraft maximum take-off mass and weight.

characteristic of aircraft performance design and analysis. The take-off mass can be determined using the unity equation by Calculating:

$$m_0 = \frac{m_{pay} + m_{FCEq}}{1 - m_{fuel} - m_{str} - m_{PP} - m_{equip}}$$

M_{pay}

WHERE: is the payload mass, which is set in the project specification;

m_{FCEq} is the cargo mass (, on-board equipment,) is the flight crew & equipment mass (flight and maintenance crew, on-board equipment, luggage and food containers), which is determined by the type of aircraft. Then I considered, considering that the airplane contains 84 passengers and 10 crew, think about the mass of the flight crew and equipment. each flight crew member, The average mass of each flight crew is 60 kg plus 10 kg of luggage. About 200 kg of equipment and food containers are on board. The mass of the flight crew and their equipment can be estimated as follows:

$$= (10+84) * (60+10) + 200 = 6780 \text{ kg}$$
$$\bar{m} = 0.3, \bar{m} = 0.1, \bar{m} = 0.1, \bar{m} = 0.1$$

Then the maximum take-off mass

$$m_0 = \frac{10500+6780}{1-0.3-0.1-0.1-0.1} = 43200\text{kg}$$

The relative error is only 3%, and the projected value is nearly identical to the design value. Thus, the estimated value may be considered the worth of the finished design. You may figure out the aircraft's take-off weight by using the formula

2.14 The Take-off Wing Loading

$$m_{land}gn_z = CL_{approach} * S * \frac{\rho_{approach}V_{approach}^2}{2}$$

$n_z = 1$ is the Applied load factor;

m_{land} is the aircraft landing mass

$$m_{land} = m_0 - m_{fuel} = m_0(1 - \bar{m}_{fuel});$$

$\rho_{approach} = 1.120 \text{ kg/m}^3$ is air density at the approach altitude;

$$CL_{max,landing}.$$

$$CL_{approach} = 1.3 CL_{max,landing}$$

Then the wind loading can be calculated as: $CL_{approach} = \frac{m_0g}{S} =$

$$\frac{CL_{max,landing}^{1.120} V_{approach}^2}{1.69 \cdot 2(1 - \bar{m}_{fuel})} = \frac{CL_{max,landing} V_{approach}^2}{3.02(1 - \bar{m}_{fuel})}, N/m^2$$

$$\text{Let } V_{approach} = \frac{230\text{km}}{h} = \frac{63.8\text{m}}{s}, CL_{max,landing} = 2.84; \bar{m}_{fuel} = 0.30$$

$$\text{Then, } \frac{W}{S} = \frac{2.84 \cdot 63.8 \cdot 63.8}{3.02(1 - 0.30)} = 5468.32 N/m^2$$

$$S = \frac{m_0g}{\left(\frac{W_0}{S}\right)} = \frac{43200 \cdot 9.8}{5468} = 77.4 m^2$$

NO	AIRCRAFT	TYPE	M_{T0} (kg)	B (M)	C_A / C	SPAN RATIO		δ_{AMAX}	
						$b_i/b/2$	$b_o/b/2$	UP	DOWN
1	Bae146	jetliner	43200	28.08	0.25	0.6	0.94	25	20

TABLE 1 designing of the roll control surface for regional jet liner that is graduation thesis aircraft bae146 in accordance with the given standard parameters and MIL-F-8785C requirements; as follows; A regional jetliner with a of **43200 kg** is classified as **Class III** based on A phase C operation is the approach flight operation. **The level of acceptance of 1** is taken into account when designing the aileron. Therefore:

CLASS	FLIGHT PHASE	LEVEL OF ACCEPTABILITY
III	C	1

Table 2 of level of acceptance The standard table, which specifies that the aircraft in Class III, flight phase C for a level of acceptability of 1, is required to be able to achieve a bank angle of 30 in 2.5 seconds, identifies the roll control handling qualities design requirement.

The inboard and outboard positions of the aileron as a function of wing span (i.e., b_i/b and b_o/b) are therefore arbitrarily chosen to be at **60% and 94%** of the wing span, respectively, in accordance with **TABLE 1-8**.

From **Table 1-8's** standard It has been decided to choose 25% as the ratio between the aileron chord and the wing chord (i.e. C_a/C).

Table 1-8 calculates the aileron efficacy parameter (a) using standards. Given that the ratio of the aileron to the wing chord is 0.25, the aileron effectiveness parameter will be 0.5

The aileron rolling moment coefficient derivative ($CL_{\delta A}$) Is calculated employing equation, $CL_{\delta A} = \frac{2cl_{aw}c_r}{sb} \left[\frac{y^2}{2} + \frac{2}{3} \left(\frac{\lambda-1}{b} \right) y^3 \right] y_0 y_1$

I have to first figure out the wing root chord, mean aerodynamic chord, and span.

From Standards $AR = 8.5$, $\lambda = 1$, $S = 26$, $cl_{aw} = 0.9$

$$\text{Therefore; } AR = \frac{B^2}{S} = b = \sqrt{S * AR} = b = \sqrt{26 * 8.5},$$

$$b=14.866$$

$$AR = \frac{b}{c} = \bar{c} = \frac{b}{AR} = \frac{14.866}{8.5} \Rightarrow \bar{c} = 1.74m$$

$$\bar{c} = \frac{2}{3} C_r \left(\frac{1 + \lambda + \lambda^2}{1 + \lambda} \right) \Rightarrow 1.74m = \frac{2}{3} C_r \left(\frac{1 + 1 + 1^2}{1 + 1} \right) \Rightarrow C_r = 1.73m$$

The inboard and outboard positions of the aileron as a function of wing span are selected to be at 60% and 94% of the wing span respectively. Therefore:

$$y_i = 0.6 * \frac{14.8}{2} \Rightarrow y_i = 4.4m$$

$$y_o = 0.94 * \frac{14.8}{2} \Rightarrow y_o = 6.956m$$

The following values should be plugged into the aileron rolling moment coefficient derivative formula

$$CL_{\delta A} = \frac{2 * 0.9 * 0.5 * 1.73}{26 * 14.8} \left(\frac{6.956^2}{2} + \frac{2}{3} \left(\frac{1-1}{14.8} \right) * 6.956^3 \right) - \left(\frac{4.4^2}{2} + \frac{2}{3} \left(\frac{1-1}{14.8} \right) * 4.4^3 \right)$$

$$0.096 - 9.68 = -9.584 \text{ deg in rad, which equate to } CL_{\delta A} = -0.165 \frac{1}{rad}$$

Control surface angle of attack effectiveness parameter

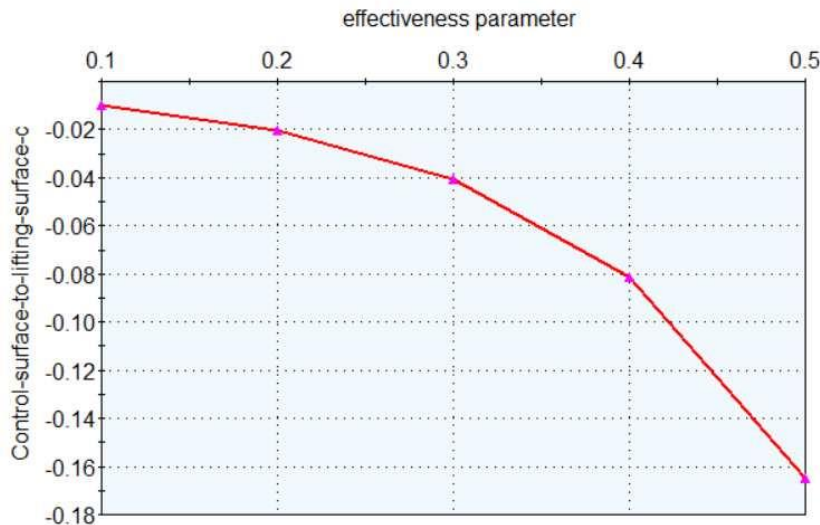


FIG 5 AILERON EFFECTIVENESS

When the aileron is deflected with the greatest deflection, the rolling moment of the airplane is determined. In most cases, the approach velocity is between 1.1 and 1.3 times the stall speed, hence the aircraft is said to be approaching at 1.3. In addition, the approach flight operation takes sea level altitude into account.

$$V_{app} = 1.3V_s = 1.3 * 110 = 143 \text{ knot} = 73.5 \frac{m}{s}$$

$$L_A = \frac{1}{2} \rho V_{app}^2 S C_l b = \frac{1}{2} * 1.225 * 73.5^2 * 26 * (-4.125) * 14.86 = -527,3474 \text{ Nm}$$

The steady-state roll rate (P_{ss}) is determined;

$$P_{ss} = \sqrt{\frac{2 \cdot L_a}{\rho(S_w + S_H + S_{VT})C_{DR}y_D}}$$

The wing-horizontal tail-vertical tail rolling drag coefficient is set to an average value of 0.9. Since it is assumed that the drag moment arm is at 405, this means that: $y_D = 0.4 \frac{b}{2} = 0.4 * \frac{14.86}{2} = 2.972 \frac{m}{s}$

$$P_{ss} = \sqrt{\frac{2 \cdot (-5273474)}{1.225(26 + 16.3 + 26.4) \times 0.9 \times (2.972)^3}} = -92 \frac{rad}{sec}$$

Aircraft bank angle response to an aileron deflection

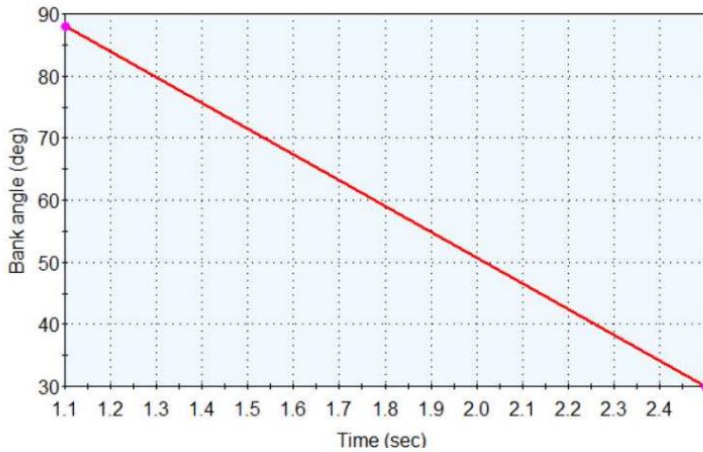


FIG 6 BANK ANGLE DEFLECTION

Calculate the bank angle (Φ_1) at which the aircraft achieves the steady state roll

$$\text{rate: } \Phi_1 = \frac{l_{xx}}{\rho y_D^3 ((S_w + S_H + S_{VT}) C_{DR})} \ln(P_{SS}^2) =$$

$$\frac{43200}{(1.225 * (2.973)^3 (26 + 16.3 + 26.4))} \ln(-92)$$

$$\Phi_1 = 88.4 \text{ rad} = 5064 \text{ deg}$$

Aircraft roll rate response to an aileron deflection

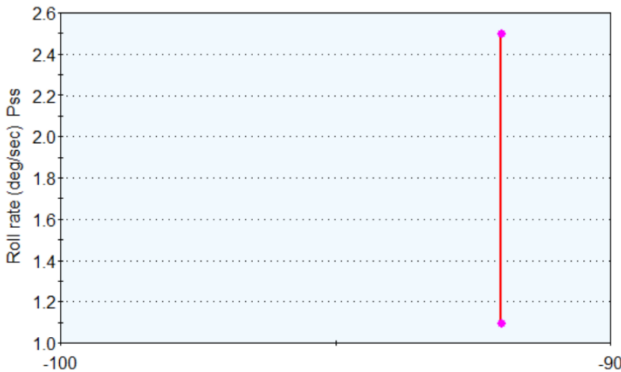


FIG 7 AIRCRAFT ROLL RATE RESPONSE

Calculate the aircraft rate of roll rate () that is produced by the aileron rolling moment until the aircraft reaches the steady-state roll rate

$$(P_{SS}). P = \frac{p_{SS}^2}{2\Phi_1} = \frac{-92^2}{2 * 88} = 48 \frac{\text{rad}}{\text{sec}^2}$$

The previously determined bank angle () and the standard bank angle () are compared. The time it takes the airplane to reach the required bank angle of 30 degrees is calculated because the bank angle (i.e., 5064 degrees) is more than the required bank angle (i.e., 30 degrees) from initial standard, we recall

$$t_2 = \sqrt{\frac{2\Phi_{des}}{p}} = \sqrt{\frac{2 * 30}{48}} = 1.1 \text{ secs}$$

The roll time obtained from standard parameters compared with the required roll time achieve the bank angle of 30 degrees 2.5secs is less than the roll time expressed 1.1secs Our aileron design satisfy the requirements Therefore we calculate the geometry for design for each aileron

$$b_A = y_{oA} - y_{iA} = 6.956 - 4.4 = 2.556mm$$

$$C_A = 0.2C_W = 0.2 * 1.74 = 0.348cm$$

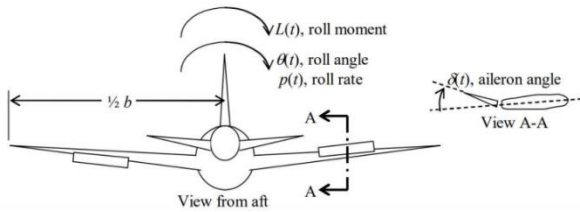
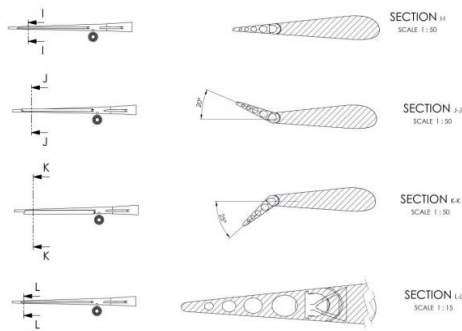


Fig 1.16 Top-view of the right-wing section The left and right ailerons' combined planform areas are: $A_A = 2b_A C_A = 2 * 2.556 * 0.34 = 1.738m^3$



For aileron effectiveness we say, as follows ;An aileron deflection ξ produces *changes* ΔL and ΔM_0 in the wing lift, L , and wing pitching moment, M_0 ; these in turn cause an elastic twist, θ , of the wing. Thus,

$$\Delta L = \frac{1}{2} \rho V^2 S \frac{\frac{1}{2} \rho v^2 \left[\left(\frac{\partial C_L}{\partial \xi} \right) e + \frac{C \partial_{M,0}}{\partial \xi} \right] \partial C_L}{k - \frac{1}{2} \rho V^2 S e \left(\frac{\partial C_L}{\partial \alpha} \right) \partial \alpha} + \frac{\partial C_L}{\partial \xi} \xi$$

Which equates to $\Delta L = \frac{1}{2} \rho V^2 S \frac{\frac{1}{2} \rho V^2 S c \left(\frac{\partial_{M,0}}{\partial \xi} \right) \frac{\partial C_L}{\partial \alpha} + k \left(\frac{\partial C_L}{\partial \alpha} \right)}{k - \frac{1}{2} \rho V^2 S e \left(\frac{\partial C_L}{\partial \alpha} \right)} \xi$ The increment of wing lift is therefore a linear function of aileron deflection and

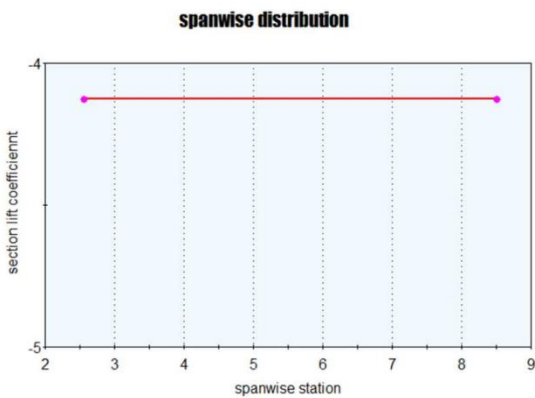


FIG 8 SPANWISE DISTRIBUTION

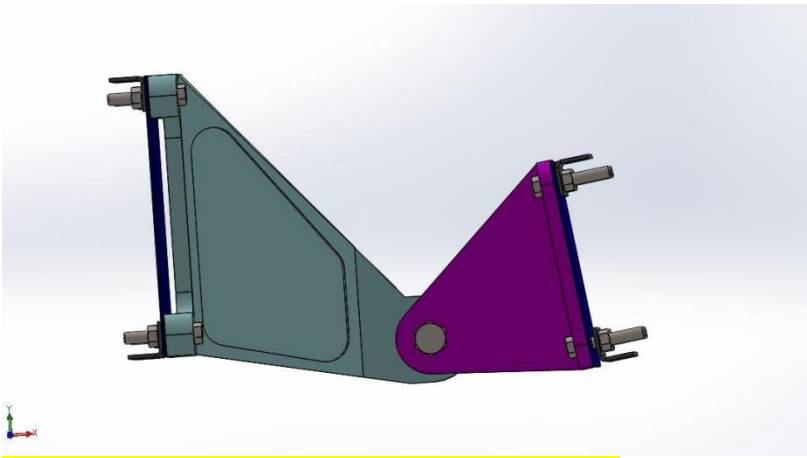


FIG 10 3D DRAWING OF AILERON ATTACHMENT

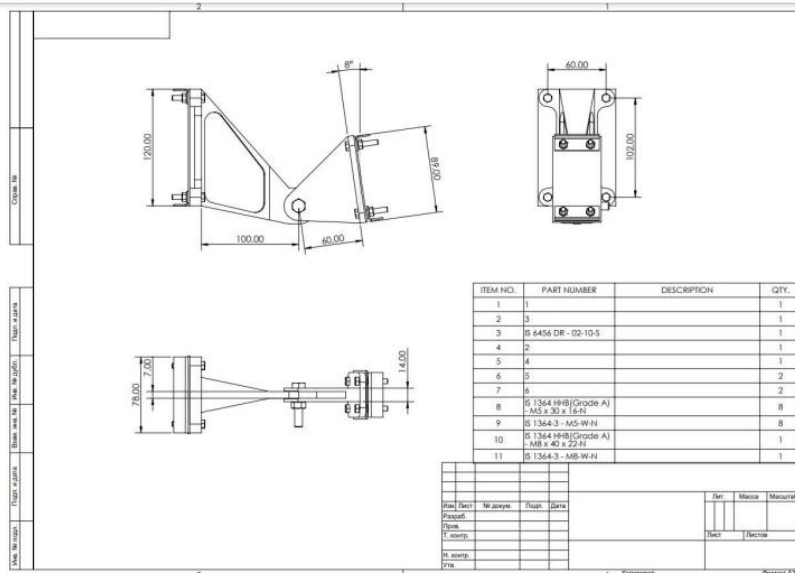


FIG11 assemble drawing of aileron attachment to wing bracket

Name	Material
<u>Details</u>	
Support bracket	D16T
Moveable bracket	D16T
Hinge	D16T
Bolt	30HGSA
<u>Standard parts</u>	
Connecting bolt	30HGSA
10-39-Z-oct 1311133-80	
Sleeve 10-24-ost 112916-77	
Sleeve 1-14-18-6-2-kd ox Ph-ost	
Nut 10cd-oct1-335048-80	
Washer 2-8-5-14-An ox oct1 345	

Table 3 summary of materials table

4. TECHNOLOGICAL SECTION

Maneuverability in aircraft production refers to the extent to which an aircraft design can be effectively and efficiently manufactured within the constraints of cost, time, and resources. It involves various considerations to ensure that the aircraft can be produced in a reliable, safe, and economically viable manner.

Environmental Considerations: As environmental sustainability becomes increasingly important, aircraft manufacturers focus on reducing the environmental impact of production processes. Efforts are made to minimize waste generation, energy consumption, and emissions by adopting eco-friendly practices and technologies.

Tooling and Equipment: The design and development of specialized tooling and equipment play a crucial role in aircraft manufacturing. Efficient tooling designs, jigs, fixtures, and automated equipment are utilized to enhance accuracy, productivity, and repeatability during production

Material	σ_b	$\sigma_{0.5}$ ($\frac{kg}{mm^2}$)	E	Technological properties
Titanium Alloy VT22	105 - 120 ($\frac{kg}{mm^2}$)	-	12000	It is well stamped and welded.
30HGSA steel	110 - 130 ($\frac{kg}{mm^2}$)	85	21000 ($\frac{kg}{mm^2}$)	Good Weldability, hot deformation, satisfactorily processed by cutting.
Aluminium T3	483 ($\frac{kg}{mm^2}$)	-	73.1GPA	has excellent fatigue resistance even though its corrosion resistance
12X18N10T steel	55 - 90 ($\frac{kg}{mm^2}$)	20	20000 ($\frac{kg}{mm^2}$)	It is well stamped in the cold state and welded.
T-39 fiberglass or reinforced fibre plastic	$[\sigma^+ 1]1800(\text{MPa})$ $[\sigma^+ 2]48(\text{MPa})$	-	$E_1 65 \text{ GPa}$ $E_2 6.3 \text{ GPa}$	high strength to weight ratio, but also reveals exceptional properties such as high durability; stiffness; damping property; flexural strength; and resistance to corrosion, wear, impact, and fire

Table 4 Materials and properties

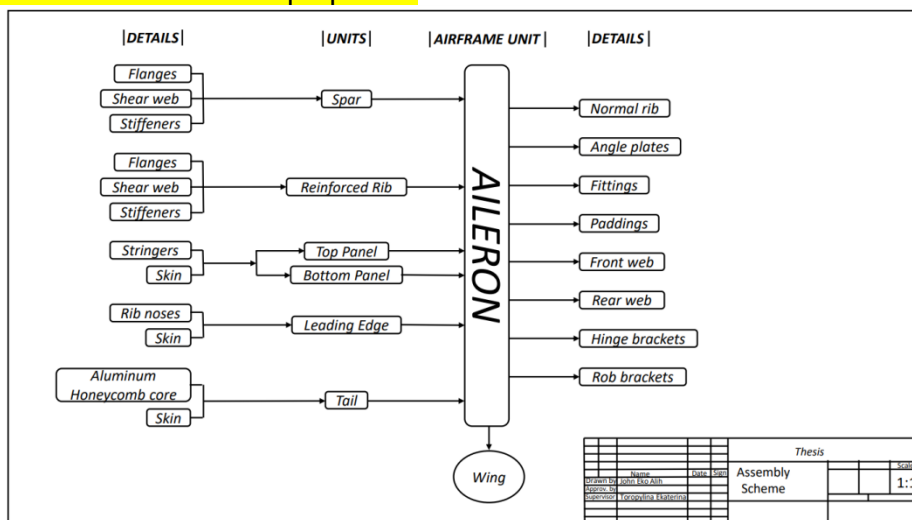


FIG 12. AILERON ATTACHMENT SCHEME [ref 6]

4.1 CONSTRUCTION DESCRIPTION

The aileron trailing edge core honeycomb plate is made of fibre reinforced plastic along the axis Spars Molded into the base-plate and his two stiffeners with foam core. The sock has a special lock.

□ Snap-in list:

- 1) matrix for making aileron
- 2) Flexible couling plate the inner surface of the panel
- 3) Rigid mandrel
- 4) Elastic couling plate
- 5) outline cropping template

□ Accessories (consumables)

- 1) Sacrificial cloth
- 2) Drainage Universal connecting elements for vacuum film
- 3) Sticky tape
- 4) Vacuum film
- 5) Sealing harness
- 6) Spiral tubes for resin supply.
- 7) Ruler for ribs
- 8) Ruler for stringers
- 9) Corner couling plate

Autoclaves: are machines used to perform industrial and scientific processes that require elevated temperatures and pressures compared to ambient pressure and/or temperature. In addition to being utilized in the chemical industry for which vulcanize rubber, laminating coatings, and synthesis by hydrothermal method, autoclaves are additionally used for per-surgical decontamination.. Industrial autoclaves are used for industrial applications, especially the production of composite materials.

PROS:

1. Economical or cheap
2. Short procedure time
3. Provides excellent penetration on all surfaces
4. No further chemicals or disposables required

CONS:

1. moisturizing power
2. Carbon steel can be damaged by moisture
3. Only heat-resistant stainless steel instruments and plastics can be sterilized.

Vacuum impregnation, also known as porous metal sealing or pore sealing, is the process of applying vacuum pressure to seal the pores in metal castings.

Vacuum impregnation is potent in removing micro- and macro-pores.

PROS of vacuum impregnation

- 1) It can prevent disassembly and cracking of parts.
- 2) Porous metal gaskets help eliminate leaks in metal castings.
- 3) Impregnation of aluminum die casting increases the overall life of metal parts.
- 4) Porous seals help reduce rejects and waste during production.

CONS of vacuum impregnation

- 1) a lot of consumables
- 2) High cost and large tank size essential are considered

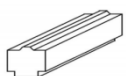


FIG 13 DIAGRAM OF MANDREL FOR STRINGER

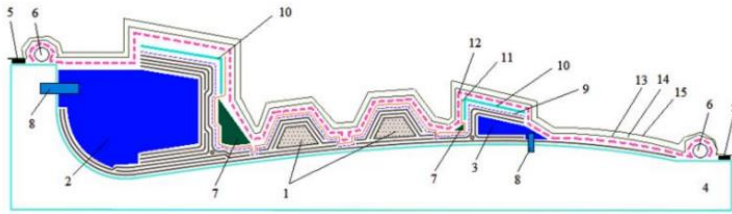


FIG 14 PACKADGE BUILD DIAGRAM

- 1-foam stringer core
- 2-rigid mandrel 1 spar
- 3-rigid mandrel 2 spars
- 4-matrix
- 5-sealing harness
- 6-drain pipe
- 7-elastic couling plate
- 8-retainer
- 9-sacrificial cloth
- 10-tsulaga of the upper shelf of the spar
- 11-perforated film
- 6212-drainage layer
- 13-inner vacuum bag
- 14 - rulers for ribs
- 15-external vacuum bag.

Snap-in requirements:

- High-temperature production (i.e., using an autoclave to create the product)
- Sealed
- Good conformity to the depicted geometry's theoretical contour Rigidity
- Impermeability

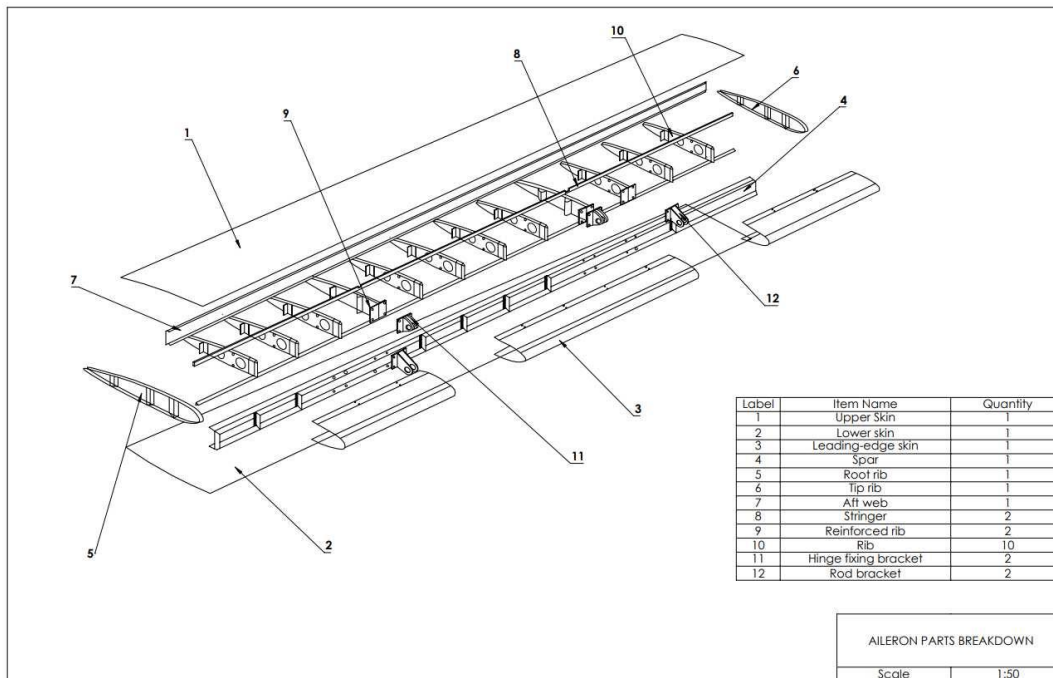


FIG 15 AILERON ASSEMBLE PARTS BREAKDOWN

5. ECONOMIC ANALYSIS

Evaluation of the cost characteristics of the technological process of manufacturing a composite aileron. The main indicators for assessing the investment attractiveness of the presented project were calculated.

- INV (Investments – necessary investments in the project);
- NPV (Net present value – Net present value);
- IRR (Internal rate of return – internal rate of return);
- PBP (Pay-back period – Payback period). Calculations of indicators for the evaluation of the investment project were carried out according to the following formulas.

FCF, \$

It is accumulated as the total of the results of operating activities and investment activities. The result of operating activities is calculated as the difference between income and expenses. The result of investment activity is calculated in the same way. The calculation is given for 4 months

DCF, \$

It is calculated as the product of the discount factor and FCF for the corresponding month. The calculation is given for 4 months
 NV, \$ It is calculated as the amount of FCF for 4 months
 NPV, \$ NPV for a period of 4 months is calculated using the following formula:

$$NPV = FCF_0 \cdot R_0 + FCF_1 \cdot R_1 + FCF_2 \cdot R_2 + FCF_3 \cdot R_3 + FCF_4 \cdot R_4$$

□ Where R- discount rate

n is the serial number of the year

The discount rate is determined by the expert method and depends on the following factors:

- the level of inflation in the country;
- the degree of risk characteristic of the object of financing;
- the increase in the value of funds over time and other factors. IRR,%

The IRR is the interest rate at which the NPV is zero. At this interest rate, the investor will be able to repay his initial investment, but no more. It is calculated as follows ;

$$0 = \frac{FCF_0}{(1+IRR)^0} + \frac{FCF_1}{(1+IRR)^1} + \frac{FCF_2}{(1+IRR)^2} + \frac{FCF_3}{(1+IRR)^3} + \frac{FCF_4}{(1+IRR)^4}$$

Figure shows the production costs.

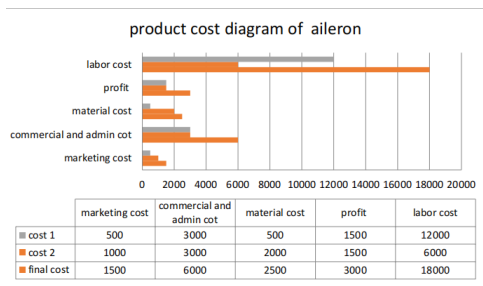


FIG 16 PRODUCTION GRAPH

After the calculations, the following results were obtained:

INV = 60000\$

NPV = 80000\$

IRR = 67%

PBP = 2

The main financial indicators of the project were calculated, the net present value is 45000 \$, the payback period is 2months

6. CONCLUSION

In the first section, the following is performed:

1. In this thesis work comparing aircraft with the main aircraft and a prototype of the main aircraft was chosen. calculation of the main characteristics of the main aircraft (take-off mass, take-off weight, starting specific load on the wing); . A drawing of the general view of the aircraft is made.
2. In the second section "preliminary design of aileron for regional airliner ", the following was also performed: 1. The loads acting on the aileron in the calculated case A were determined; . Plots of bending and shear force are constructed.
- 3 Normal and tangential stresses are determined, calculation of buckling of spar, stringer, and calculation and 3d assembly of aileron hinge attachment bracket, also drawing of aileron assembly
4. Technological section A drawing of the aileron structural parts , and exploded view of my aircraft "Technological section", the work on determining the technological process of assembly of the unit is completed, and the scheme of dividing the aircraft is also performed. In the section
5. Economic analysis and estimation of aileron maneuverability and composite manufacturing

Disclaimer

This paper is an extended version of a Thesis document of the same author.

The Thesis document is available in this link:

https://www.academia.edu/105436556/PRELIMINARY_STRUCTURAL_DESIGN_OF_REGIONAL_JET_AILERON

[As per journal policy, Thesis article can be published as a journal article, provided it is not published in any other journal]

Authors' contributions

This work was carried out in collaboration among all authors. All authors read and approved the final manuscript

Disclaimer (Artificial intelligence)

Option 1:

Author(s) hereby declare that NO generative AI technologies such as Large Language Models (ChatGPT, COPILOT, etc) and text-to-image generators have been used during writing or editing of manuscripts.

Option 2:

Author(s) hereby declare that generative AI technologies such as Large Language Models, etc have been used during writing or editing of manuscripts. This explanation will include list the name, version, model, and source of the generative AI technology and as well as the all input prompts provided to a generative AI technology

Details of the AI usage are given below:

- 1.
- 2.
- 3.

REFERENCES

1. Warwick, Graham (14 September 2012). "Crunching Gravel Down Under". Aviation Week & Space Technology. Archived from the original on 8 March 2014. Retrieved 20 September 2012.
2. "hawker siddeley - flight international - series - 1973 - 2582 - Flight Archive".

3. "World Airliners". Flight International. 28 August 2001
4. (1 June 2020). Bombardier Concludes Sale of the CRJ Series Regional Jet Program to Mitsubishi Heavy Industries - Bombardier (in en). Press release . Archived from the original on 11 December 2020. Retrieved 2021-01-01
5. Avco Lycoming Division (July 1970). "Proven power, turbofan or turboprop, for any AX configuration". Air Force Magazine. p. 45
6. Type certificate data sheet E6NE" (15th ed.). Department of Transportation, Federal Aviation Administration (FAA). June 7, 2002.
7. 92 pages September 2012, Hardcover Wiley Publications
8. Aircraft Structures for Engineering Students (Fifth Edition), 2013
9. Vasiliev V. V. "Fundamentals of design and manufacture of aircraft structures made of composite materials". - Moscow: MAI, 1985. – 218p
10. Dudchenko A. A. "Strength and design of elements of aircraft structures made of composite material". - M.: MAI Publishing House, 2007. – 200p.
11. Voit E. S., Endogur A. I., Melik-Sarkisyan Z. A., Alyavdin I. M. Design of aircraft structures: Textbook P79 for university students studying in the specialty "Aircraft construction". Moscow: Mashinostroenie, 1987 - 416 p.
12. "the definition of labour". Dictionary.com. Retrieved 2017-03-09.
13. "Environment | Define Environment at Dictionary.com". Retrieved 2017-03-09.
14. EASA CS-25 - "Certification Specifications for Large Aeroplanes" - European standards for the certification of large aircraft.
15. SAE ARP4754A - "Guidelines for Development of Civil Aircraft and Systems" - Provides guidelines for the development of civil aircraft systems, including structural components.
16. "Preliminary Design of Aircraft Ailerons Using Advanced Materials" by Lisa Martin et al., AIAA Aviation Forum, 2017 - Discusses the preliminary design process using advanced materials.
17. "Structural Integrity of Aircraft Control Surfaces" by David Johnson et al., ICAS Congress, 2018 - Covers structural integrity considerations for control surfaces.
18. "Lightweight Design of Aircraft Ailerons" by Susan Lee et al., SAE AeroTech Congress, 2019 - Focuses on lightweight design techniques for ailerons.
19. "Innovative Manufacturing Techniques for Aircraft Ailerons" by Paul Wilson et al., SAMPE Conference, 2020 - Discusses new manufacturing techniques for aileron production.
20. "Advanced Simulation Techniques for Aircraft Aileron Design" by Mark Taylor et al., AIAA SciTech Forum, 2021 - Explores advanced simulation methods for aileron design.
21. NASA Technical Report - "Design and Analysis of Aircraft Ailerons" by JPL Team, 2016 - Provides insights from NASA's research on aileron design.
22. NACA Report - "Aerodynamic and Structural Analysis of Aircraft Control Surfaces" by NACA Team, 1950 - Historical reference with fundamental aerodynamic and structural analysis methods.
23. Boeing Technical Report - "Composite Material Applications in Aircraft Ailerons" by Boeing Research Team, 2018 - Discusses Boeing's research and application of composites in aileron design.
24. Airbus Technical Report - "Structural Optimization of Aircraft Control Surfaces" by Airbus Engineering Team, 2019 - Details Airbus's approach to structural optimization in control surfaces.
25. Lockheed Martin Technical Report - "Advanced Materials and Design Techniques for Aircraft Ailerons" by Lockheed Martin R&D, 2020 - Explores the use of advanced materials and design techniques for ailerons.
26. Ayeni BK, Yisah SO. Cloud Based Architecture Solution for Aircraft Flight Data Recorder. Curr. J. Appl. Sci. Technol. [Internet]. 2015 Nov. 16 [cited 2024 May 28];13(2):1-13. Available from: <https://journalcjust.com/index.php/CJAST/article/view/47>
27. Siqueira LFR, Sousa MS de, Cardoso-Ribeiro FL, Junior SS da C. A Detailed Physical Explanation of an Aircraft Flutter Mechanism. Arch. Curr. Res. Int. [Internet]. 2024 May 1 [cited 2024 May 28];24(5):191-212. Available from: <https://journalacri.com/index.php/ACRI/article/view/696>

28 Ritter M. Nonlinear numerical flight dynamics of flexible aircraft in the time domain by coupling of CFD, flight mechanics, and structural mechanics. In *New Results in Numerical and Experimental Fluid Mechanics VIII: Contributions to the 17th STAB/DGLR Symposium Berlin, Germany 2010 2013* (pp. 339-347). Springer Berlin Heidelberg.